REPORT SSD-TR-90-03

A Survey of Equatorial Magnetospheric Wave Activity Between 5 and 8 R_E

H. C. KOONS and J. L. ROEDER
Space Sciences Laboratory
Laboratory Operations
The Aerospace Corporation
El Segundo, CA 90245-4691

1 March 1990

Prepared for

SPACE SYSTEMS DIVISION
AIR FORCE SYSTEMS COMMAND
Los Angeles Air Force Base
P.O. Box 92960
Los Angeles, CA 90009-2960

This report was submitted by The Aerospace Corporation, El Segundo, CA 90245, under Contract No. F04701-88-C-0089 with the Space Systems Division, P.O. Box 92960, Los Angeles, CA 90009-2960. It was reviewed and approved for The Aerospace Corporation by H. R. Rugge, Director, Space Sciences Laboratory.

Lt Tyron Fisher was the project officer for the Mission-Oriented Investigation and Experimentation (MOIE) Program.

This report has been reviewed by the Public Affairs Office (PAS) and is releasable to the National Technical Information Service (NTIS). At NTIS, it will be available to the general public, including foreign nationals.

This technical report has been reviewed and is approved for publication. Publication of this report does not constitute Air Force approval of the report's findings or conclusions. It is published only for the exchange and stimulation of ideas.

TYRON FISHER, LT, USAF
MOIE Project Officer
SSD/CLFPO

RAYMOND M. LEONG, MAJ, USAF
MOIE Program Manager
AFSTC/WCO OL-AB

UNCLASSIFIED

SECURITY CLASSIFICATION OF THIS PAGE

REPORT DOCUMENTATION PAGE

1a. REPORT SECURITY CLASSIFICATION Unclassified	1b. RESTRICTIVE MARKINGS
2a. SECURITY CLASSIFICATION AUTHORITY	3. DISTRIBUTION/AVAILABILITY OF REPORT Approved for public release; distribution unlimited.
2b. DECLASSIFICATION/DOWNGRADING SCHEDULE	
4. PERFORMING ORGANIZATION REPORT NUMBER(S) TR-0089(4940-06)-2	5. MONITORING ORGANIZATION REPORT NUMBER(S) SSD-TR-90-03
6a. NAME OF PERFORMING ORGANIZATION The Aerospace Corporation Laboratory Operations 6b. OFFICE SYMBOL (If applicable)	7a. NAME OF MONITORING ORGANIZATION Space Systems Division
6c. ADDRESS (City, State, and ZIP Code) El Segundo, CA 90245-4691	7b. ADDRESS (City, State, and ZIP Code) Los Angeles Air Force Base Los Angeles, CA 90009-2960
8a. NAME OF FUNDING/SPONSORING ORGANIZATION 8b. OFFICE SYMBOL (If applicable)	9. PROCUREMENT INSTRUMENT IDENTIFICATION NUMBER F04701-88-C-0089
8c. ADDRESS (City, State, and ZIP Code)	10. SOURCE OF FUNDING NUMBERS PROGRAM ELEMENT NO. / PROJECT NO. / TASK NO. / WORK UNIT ACCESSION NO.

11. TITLE (Include Security Classification)

A SURVEY OF EQUATORIAL MAGNETOSPHERIC WAVE ACTIVITY BETWEEN 5 AND 8 R_E

12. PERSONAL AUTHOR(S)

Koons, Harry C., and Roeder, James L.

13a. TYPE OF REPORT	13b. TIME COVERED	14. DATE OF REPORT (Year, Month, Day)	15. PAGE COUNT
	FROM _____ TO _____	1990 March 1	27

16. SUPPLEMENTARY NOTATION

17. COSATI CODES			18. SUBJECT TERMS (Continue on reverse if necessary and identify by block number)
FIELD	GROUP	SUB-GROUP	Diffuse aurora Plasma waves Whistler chorus

19. ABSTRACT (Continue on reverse if necessary and identify by block number)

We report the results of a survey of ELV/VLF wave activity in the frequency range from 100 Hz to 5 kHz observed by the SCATHA satellite near the magnetic equator between 5 and 8 R_E. The typical wave environment in this region is required to assess the role of each type of wave in transport processes, such as the pitch-angle diffusion of electrons, occurring in the outer magnetosphere. Hiss, discrete whistler-mode emissions, and electron cyclotron harmonic waves occur within the frequency range of the SCATHA VLF receiver. Hiss is predominantly observed between noon and dusk where the satellite frequently enters the plasmasphere. Discrete whistler-mode emissions occur over 60% of the time between 0300 and 1200 LT. A surprising result of the survey is the absence of activity in the local time sector from 18 to 21 h. No wave activity above the receiver noise level, 5×10^{-7} V/m-Hz$^{1/2}$, was detected during 50% of the broadband data acquisitions in this region.

20. DISTRIBUTION/AVAILABILITY OF ABSTRACT	21. ABSTRACT SECURITY CLASSIFICATION
☐ UNCLASSIFIED/UNLIMITED ☒ SAME AS RPT. ☐ DTIC USERS	Unclassified
22a. NAME OF RESPONSIBLE INDIVIDUAL	22b. TELEPHONE (Include Area Code) / 22c. OFFICE SYMBOL

DD FORM 1473, 84 MAR

83 APR edition may be used until exhausted.
All other editions are obsolete

SECURITY CLASSIFICATION OF THIS PAGE

UNCLASSIFIED

PREFACE

We are indebted to L. Friesen, R. Maulfair, and J. Kordan for providing support of the data reduction and analysis.

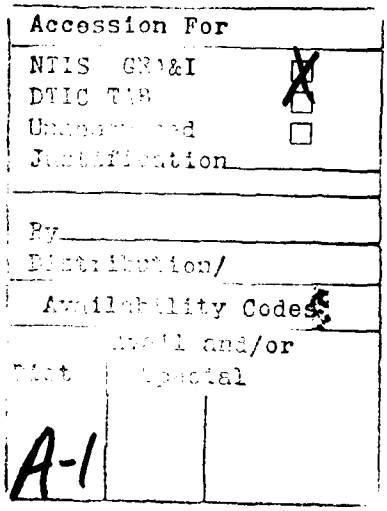

CONTENTS

FIGURES

I. INTRODUCTION

A variety of plasma wave emissions is routinely detected by the VLF receiver aboard the SCATHA (P78-2) satellite. In the course of a year, this satellite provides complete coverage of the radial range from 5 to 8 R_E at low inclination. This is an important region because it covers a significant portion of the outer radiation belt and because the geomagnetic field lines passing through this region connect with the auroral zone. Chorus emissions are generated here when newly injected substorm electrons drift around the dawn side of the earth. Electron cyclotron harmonic (ECH) emissions are observed in the outer portion of the range, and strong hiss emissions are detected when the spacecraft enters the plasmasphere on the dusk side of the earth. In this report we discuss the results of a survey of wave activity based on 1 year of data from the broadband VLF receiver.

II. BROADBAND VLF WAVE DATA

The SCATHA (P78-2) satellite was launched on January 30, 1979, into an equatorial orbit with a 23 h, 35 m period, a 7.9 deg inclination, a 7.78 R_E apogee, and a 5.32 R_E perigee. The VLF receiver on board has both narrow band and broadband channels. The receiver uses two antennas: an air-core loop detects the magnetic component of waves, and a 100-m tip-to-tip dipole, provided by the Goddard Space Flight Center for their DC Electric Field Experiment, detects the electric component.

The sensitivity of the electric field receiver is 5×10^{-7} V/m-Hz$^{1/2}$ at 1.3 kHz and 10^{-7} V/m-Hz$^{1/2}$ at 10.5 kHz. The air-core loop is electrostatically shielded and has an effective area of 575 m^2 at 1.3 kHz. The sensitivity of the magnetic field receiver is 3×10^{-6} γ/Hz$^{1/2}$ at 1.3 kHz. The receiver has eight narrow band channels between 400 Hz and 300 kHz. There are also two broadband modes, 100 Hz to 3 kHz and 100 Hz to 5 kHz. An automatic gain control (AGC) circuit for the broadband channel provides a dynamic range of approximately 60 dB. The receiver processes signals from only one of the antennas at a time. Its input is normally switched between the electric and the magnetic antennas every 16 s.

Only the broadband data were used for this survey. The broadband data can only be collected in real time by a telemetry ground station. One to 2 h of broadband data were collected each day during 1979 and 1980. An atlas of VLF spectrograms from each broadband data acquisition during 1979 has been compiled by Koons et al. [1981]. This collection contains samples of each type of signal detected during a given data acquisition, which generally lasted from 10 min to 1 h. For example, if hiss was detected at the beginning of an acquisition, and electron cyclotron harmonic emissions at the end of the acquisition, there would be two photographs in the album. The spectrograms were categorized by the type of wave activity present. Typical examples of the categories are shown in Fig. 1. The categories are hiss (Fig. 1a), discrete whistler-mode emissions such as chorus (Fig. 1b), lightning generated whistlers (Fig. 1c), and electron cyclotron harmonic emissions (Fig. 1d). A database was compiled with a unique record for each acquisition. A total of 813 acquisitions are contained in the database. Each record

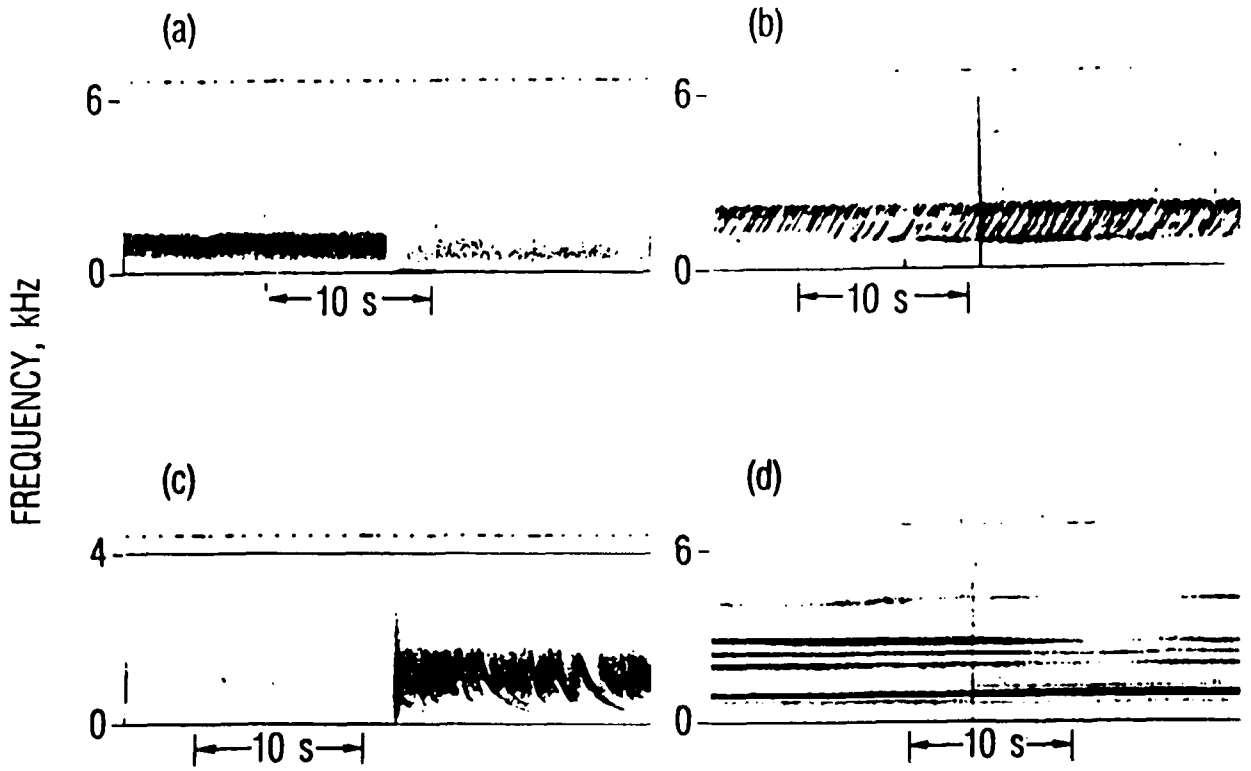

Fig. 1. Spectrograms from the SCATHA VLF Receiver. (a) Hiss emissions detected from 1614 to 1658 UT on May 14, 1979. The satellite was at a radial distance of 5.3 R_E near 1400 local time. (b) Chorus emissions detected from 1653 to 1740 UT on September 21, 1979. The satellite was at a radial distance of 6.3 R_E near 1230 local time. (c) Whistlers detected from 0200 to 0228 UT on June 16, 1980. The satellite was at a radial distance of 5.3 R_E near 1400 local time. (d) Electron cyclotron harmonic emissions detected from 1554 to 1611 UT on April 16, 1979. The satellite was at a radial distance of 5.3 R_E near 1400 local time.

contains logical fields that indicate the presence or absence of each type of wave for each acquisition. The assessment of the occurrence was made visually from the spectrograms. The sensitivity of the spectrograms is a few decibels above the noise level of the instrument.

III. SPATIAL DISTRIBUTION MAPS

Figure 2 shows the local time coverage of the broadband VLF data. The range of radii from 5 to 8 R_E is divided into six equal bins of 0.5 R_E each, and the local time is divided into eight bins of 3 h each. The coverage is greater than 15 h per bin in most of the bins. The dusk side from noon to midnight is covered somewhat better than the dawn side.

The significance of the occurrences plotted in the later figures, of course, depends on the amount of data collected in each bin. Bins with less than 10 h of coverage, such as those at the lower altitudes around midnight and at the higher altitudes before noon, have the least significance. We have chosen to retain those bins in the occurrence maps to avoid visual holes in the plots. However, these regions should not be emphasized when interpreting the data.

A. NO WAVE ACTIVITY

During 33% of the data acquisitions, no wave activity whatsoever was visible on the spectrograms. Although this is due, in part, to the limited frequency range of the survey, the consequences of a lack of activity in the hiss, chorus, and ECH modes are sufficiently important that we have made a map (Fig. 3) of the occurrence of no wave activity at all. The lack of activity is especially noticeable from 1800 to 2100 LT over the entire radial range covered by SCATHA. Over 50% of the acquisitions in this region showed no wave activity, with some bins showing no activity over 70% of the time.

B. WHISTLER-MODE EMISSIONS

We have divided whistler-mode emissions into three categories. Band-limited incoherent emissions are classified as hiss. Lightning-generated whistler-mode waves are simply called whistlers, and other whistler-mode emissions showing complex structure on the spectrograms are classified as discrete emissions or chorus. There is no evidence in the SCATHA data [Koons, 1985] for power line harmonic radiation or emissions that have been attributed to interactions with power line radiation [Helliwell et al., 1975].

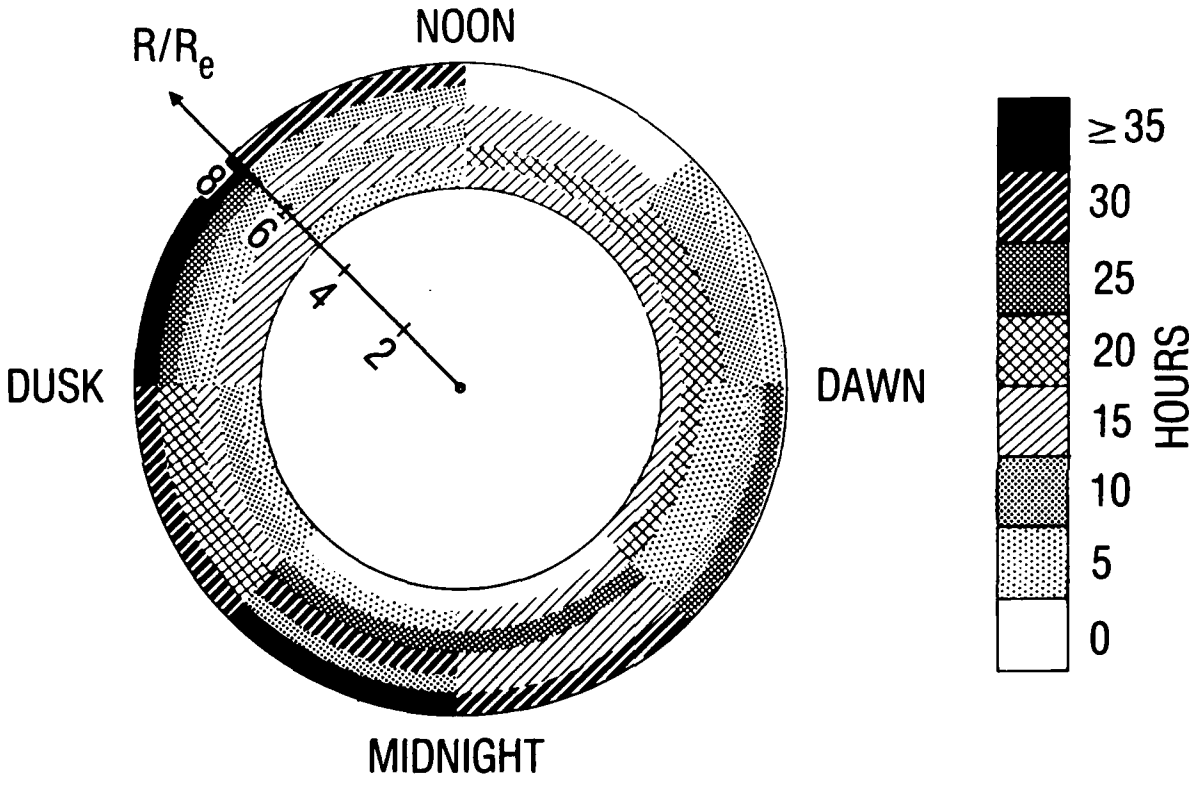

Fig. 2. Temporal Coverage by the Broadband VLF Receiver on the SCATHA Satellite as a Function of L and Magnetic Local Time. The radial range from 5 to 8 R_E is divided into six equal bins, and the local time is divided into eight equal bins.

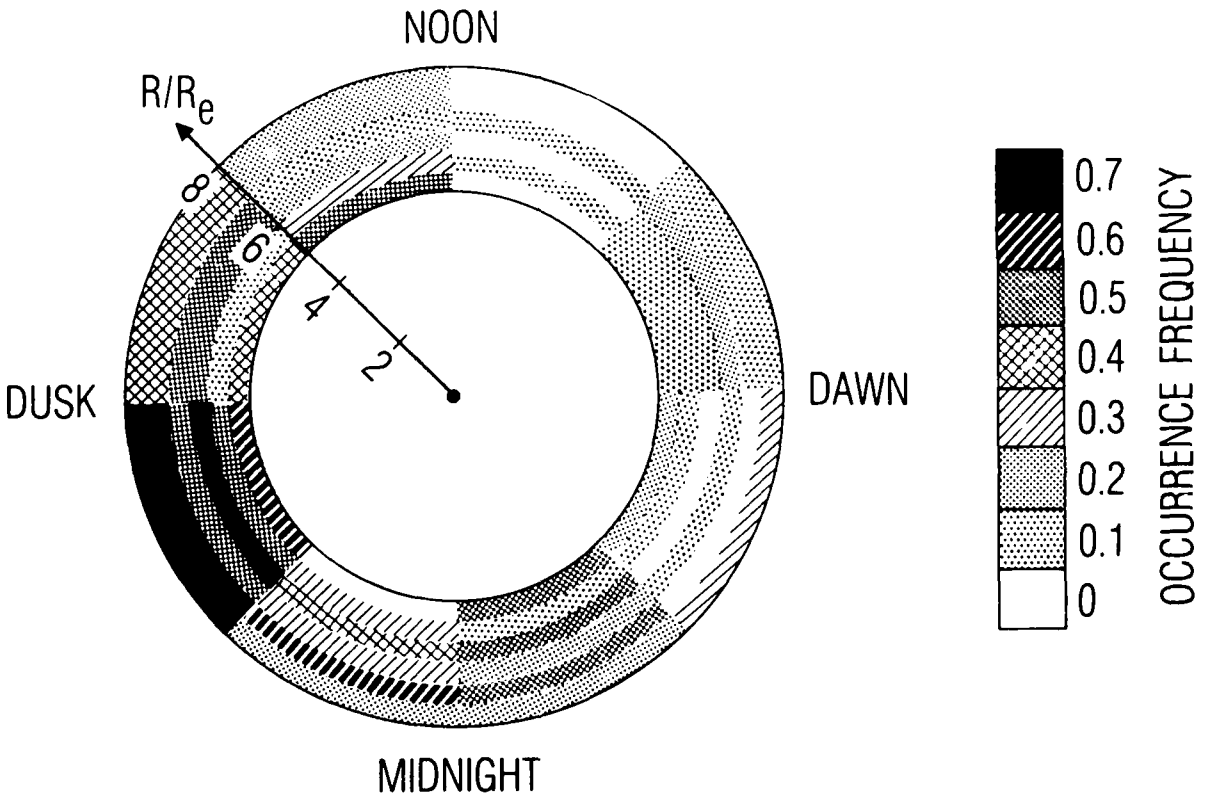

Fig. 3. Frequency of Occurrence of No Wave Activity Above the Threshold of the SCATHA Broadband VLF Receiver as a Function of Radius and Local Time

1. HISS

Figure 4 shows the distribution of hiss in the region covered by this survey. Hiss primarily occurs in the sector from noon to dusk. It is most prominent in the 400 Hz channel of the narrow band analyzer. This spatial distribution is determined by the relationship of the satellite orbit to the plasmasphere. The spacecraft orbit is within the plasmasphere only during the afternoon. The spacecraft was within the plasmasphere for many of the data acquisitions in this region. Hiss within the plasmasphere in this frequency range is commonly referred to as plasmaspheric hiss [Echeto et al., 1973].

Hiss is detected at moderately low occurrence levels at all local times at the lower range of altitudes sampled by SCATHA. The distribution of hiss may be severely distorted by the automatic gain control of the receiver. Hiss is normally much weaker than the discrete whistler-mode emissions such as chorus. When essentially continuous chorus emissions are present, such as the example in Fig. 1b, hiss is suppressed by the AGC. Cornilleau-Wehrlin et al. [1978] and Koons [1981] have shown that hiss and chorus are frequently present simultaneously, and both argue that hiss plays an important role in the generation of chorus. If that is the case, then the distribution of hiss shown in Fig. 4 is actually the distribution of hiss in the absence of chorus. Hiss may also be present over much of the region where chorus is observed (Fig. 5).

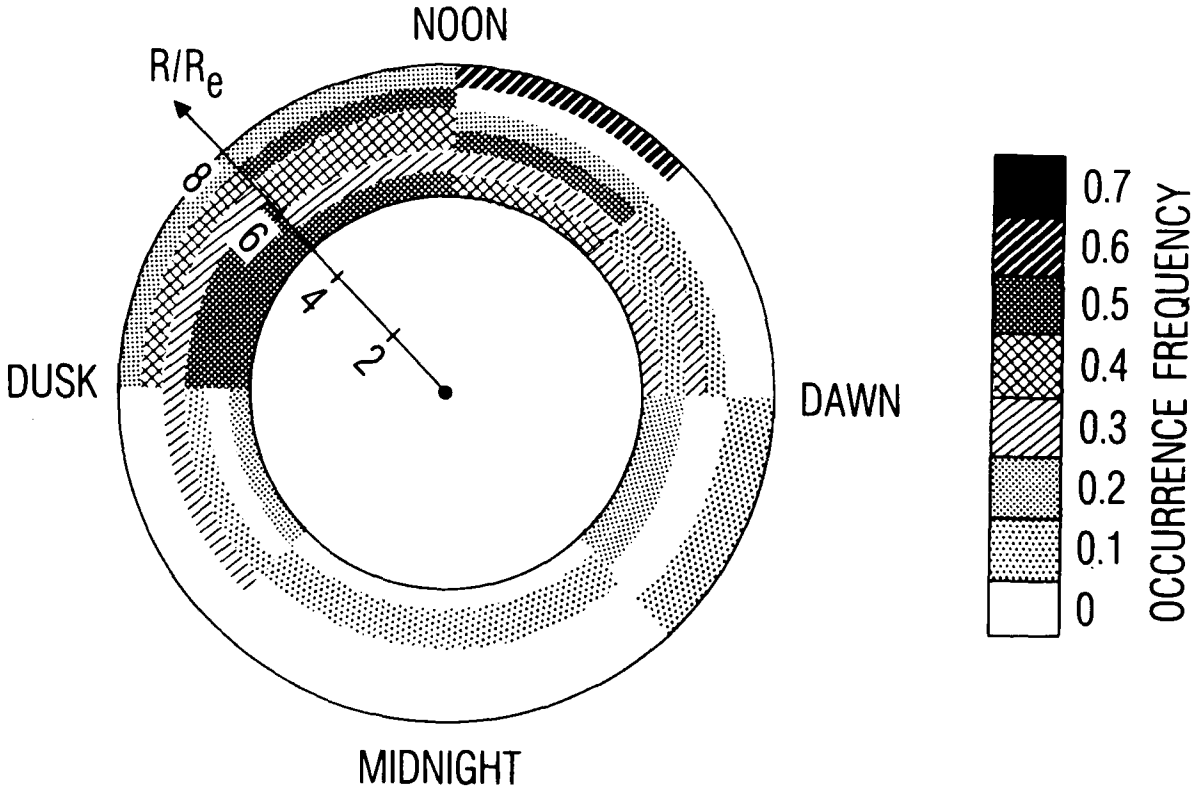

Fig. 4. Frequency of Occurrence of Hiss Emissions as a Function of Radius and Local Time

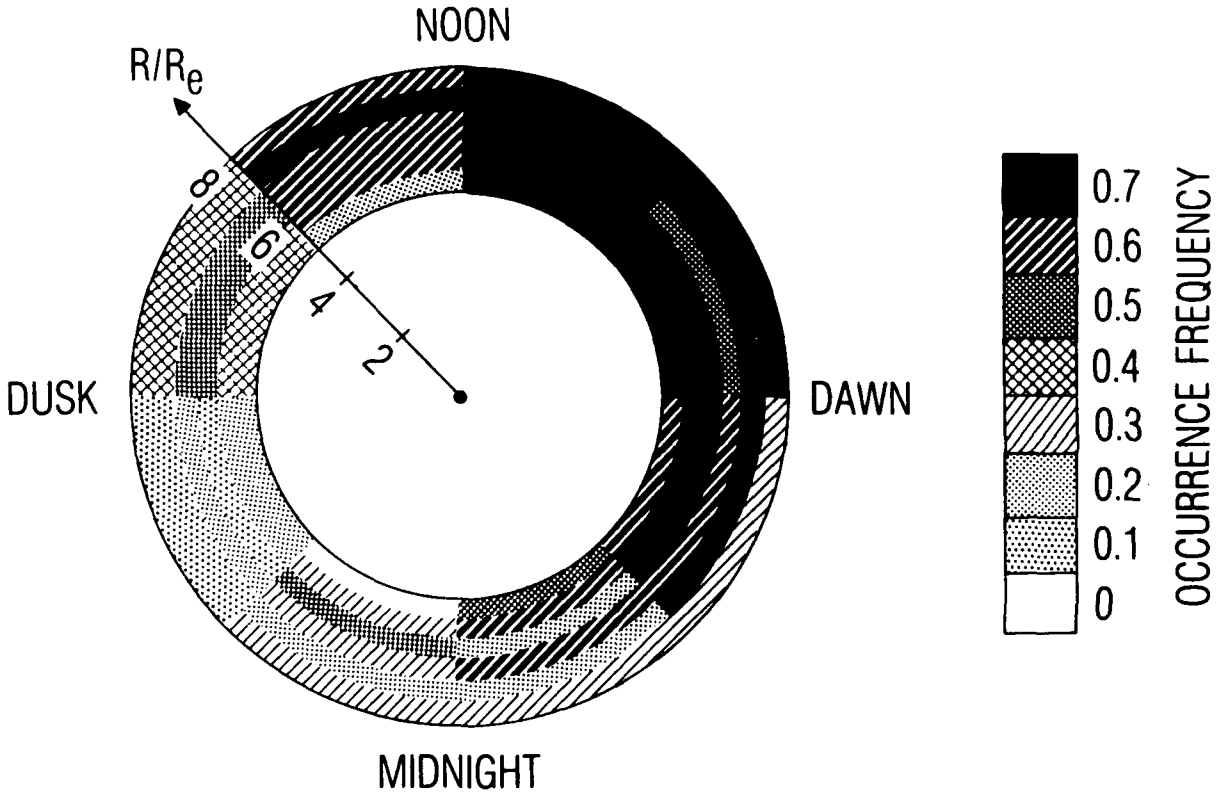

Fig. 5. Frequency of Occurrence of Chorus Emissions as a Function of Radius and Local Time

2. CHORUS

Chorus emissions are whistler-mode emissions that are commonly observed outside of the plasmasphere [Burtis and Helliwell, 1976; Tsurutani and Smith, 1974, 1977]. They are characterized as discrete emissions usually rising in frequency with time, at least at the beginning of the emission. Tsurutani and Smith [1977] have mapped the spatial distribution of chorus from L = 4 to L = 15. They note a sharp onset of chorus just postmidnight from L = 5 to L = 8, with a maximum occurrence of 54%. They detected no equatorial chorus from 1600 to 2400 LT. The occurrence map for the distribution of chorus observed by SCATHA is shown in Fig. 5. SCATHA detected chorus at all local times within the altitude range of this survey. The frequency of occurrence from dawn to noon was greater than 70%, significantly higher than that reported by Tsurutani and Smith. The spatial maps of chorus from the SCATHA satellite and the OGO satellites are similar, with SCATHA data generally showing a higher percent occurrence at all local times than the OGO data. This may be attributed to the sensitivity of the receivers. The SCATHA receiver has a peak sensitivity of 3×10^{-6} $\gamma/Hz^{1/2}$ at 3 kHz, while the OGO receivers have a peak sensitivity of 5×10^{-5} $\gamma/Hz^{1/2}$ [Tsurutani and Smith, 1977].

3. CHORUS GAP

Chorus emissions generally start in frequency between 0.1 and 0.3 ω_b, where ω_b is the electron gyrofrequency, and rise to 0.7 or 0.8 ω_b. If chorus extends above 0.5 ω_b, a gap is generally observed around 0.5 ω_b. The width of the gap is highly variable, sometimes reaching 0.2 ω_b and sometimes, but rarely, vanishing entirely. Figure 6 shows several examples of chorus displaying the full range of gap variability from slight to pronounced. Several theories have been proposed to account for the gap. The proposed mechanisms fall into two categories: (1) propagation effects [Tsurutani and Smith, 1974; Burtis and Helliwell, 1976] and (2) emission effects [Maeda, 1976; Curtis, 1978; Kaiser, 1979]. Figure 7 shows the spatial distribution of chorus containing a gap at 0.5 ω_b. It generally follows the same spatial distribution as all chorus (Fig. 5), with a reduced frequency of occurrence. In the context of this survey, chorus without a gap consists of discrete whistler mode emissions below 0.5 ω_b that are not associated with any whistler-mode emissions above 0.5 ω_b.

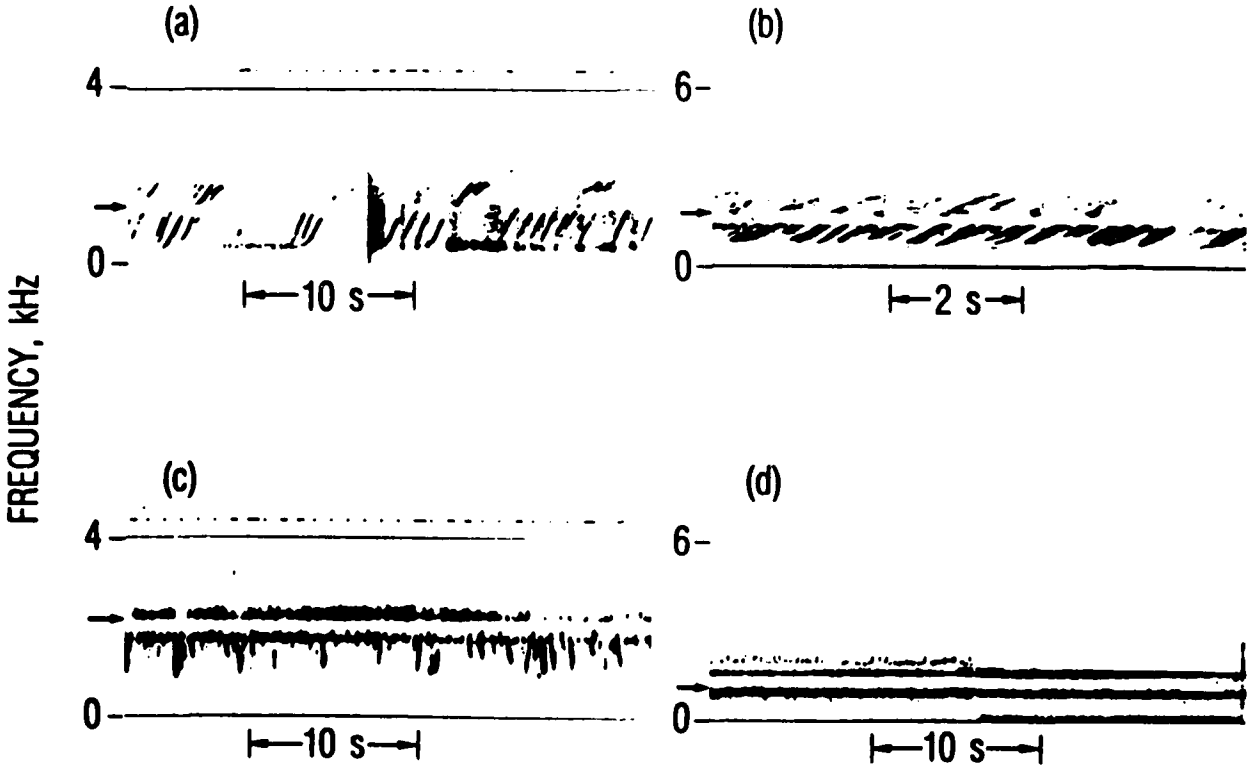

Fig. 6. Spectrograms from the SCATHA VLF Receiver of Chorus Emissions Displaying a Frequency Gap at One-half the Local Electron Gyrofrequency. (a) Emissions detected from 1531 to 1613 UT on September 29, 1979. The satellite was at a radial distance of 6.9 R_E near 1400 local time. (b) Emissions detected from 2342 on April 14, to 0010 UT on April 15, 1979. The satellite was at a radial distance of 6.5 R_E near 1015 local time. (c) Emissions detected from 0603 to 0641 UT on August 4, 1979. The satellite was at a radial distance of 5.5 R_E near 0700 local time. (d) Emissions detected from 1101 to 1145 UT on December 30, 1979. The satellite was at a radial distance of 7.5 R_E near 1430 local time. The arrow on each frequency scale points to one-half the local electron gyrofrequency.

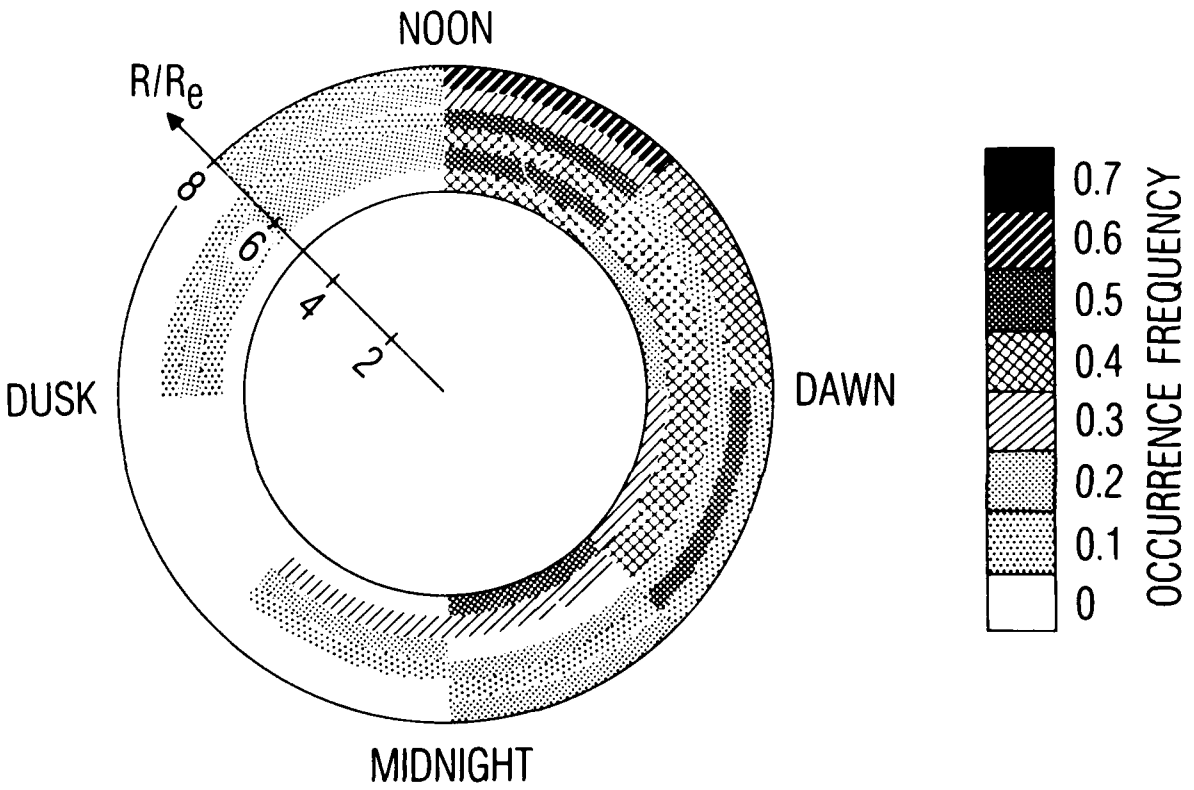

Fig. 7. Frequency of Occurrence of Chorus Emissions Displaying a Frequency Gap at One-half the Local Electron Gyrofrequency as a Function of Radius and Local Time

4. LIGHTNING GENERATED WHISTLERS

Lightning generated whistlers are rarely present in the broadband data from the SCATHA satellite. Only 5 broadband data acquisitions in 1979 and 17 in 1980 showed examples of lightning generated whistlers [Koons, 1985]. The whistlers that were detected occurred during local afternoon and evening at the lower range of radii covered by the satellite orbit. They were also predominantly detected during the Northern Hemisphere summer season. The satellite was most likely within the plasmasphere each time the whistlers were detected. The SCATHA data have convincingly shown that lightning generated whistlers are rarely detected near the equatorial plane in the outer magnetosphere.

C. ELECTRON CYCLOTRON HARMONIC WAVES

Roeder and Koons [1989] reported a survey of the spatial distribution of ECH waves observed by the AMPTE-IRM and SCATHA satellites. For completeness, Fig. 12 from that paper, showing the spatial distribution of ECH waves as observed by the SCATHA satellite, is included here as Fig. 8. It shows that ECH waves occurred relatively infrequently and only above a radius of 6 R_E from 2100 to 0900 LT.

Strong ECH waves are closely confined to the magnetic equator [Christiansen et al., 1978; Gough et al., 1979]. Although the data in Fig. 8 are not sorted by magnetic latitude, they were predominantly taken at low magnetic latitudes. The survey contains 813 samples (data acquisitions). Thirty-nine percent are below 5 deg magnetic latitude, and 67% are below 10 deg magnetic latitude.

ECH emissions in the outer magnetosphere are often cited as the pitch angle scattering mechanism responsible for the diffuse auroral precipitation [Kennel and Ashour-Abdalla, 1982]. The generally low frequency of occurrence for ECH waves shown in Fig. 8 may have important implications for the theory of the diffuse aurora.

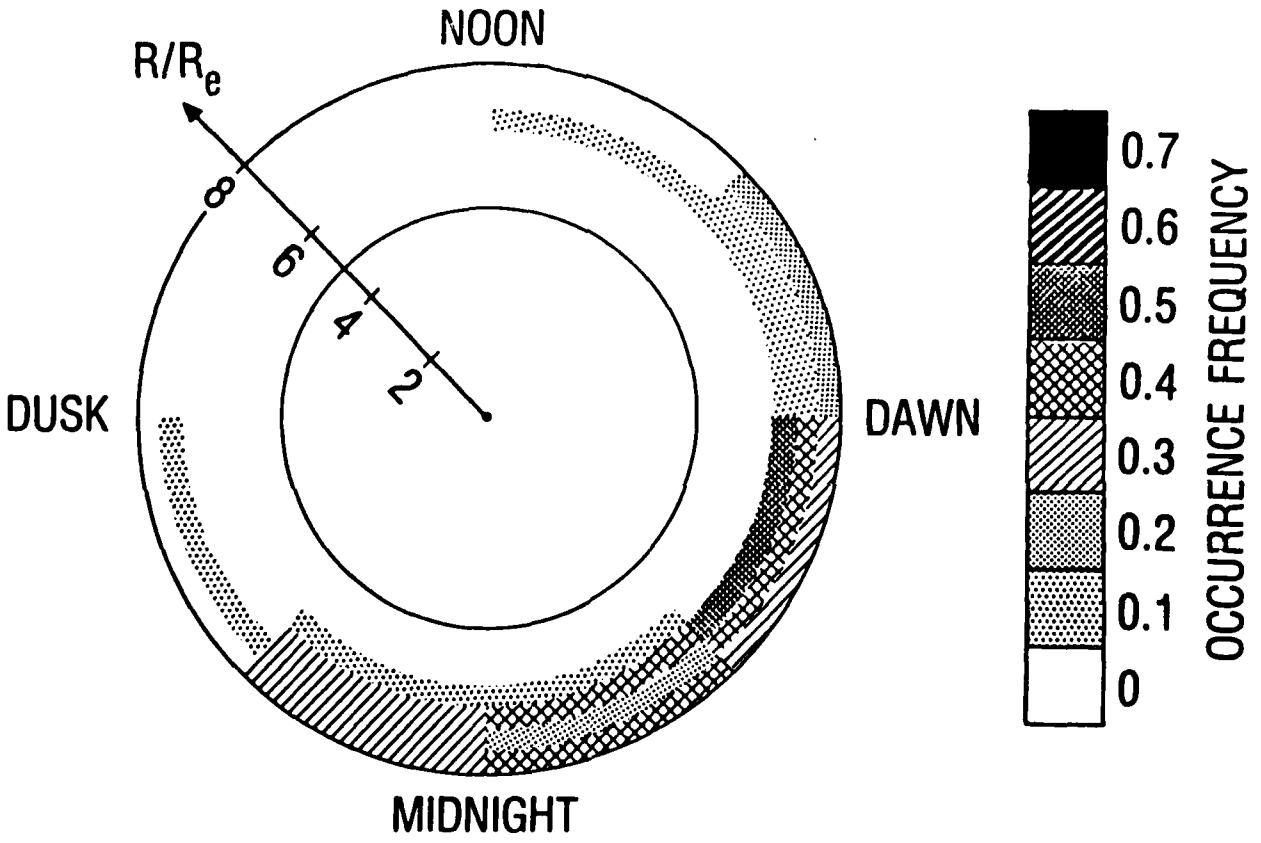

Fig. 8. Frequency of Occurrence of Electron Cyclotron Harmonic Emissions as a Function of Radius and Local Time

D. UPPER HYBRID WAVES

The upper cutoff frequency, 5 kHz, for this survey is too low to observe the electrostatic waves that have been reported at the upper hybrid frequency. Kurth et al. [1979] report intense waves at the upper hybrid resonance frequency occurring just outside the plasmapause about 10% of the time. Mosier et al. [1973] report similar observations inside of the plasmasphere.

IV. CONCLUSIONS

We have presented spatial distribution maps showing the occurrence of a variety of ELF/VLF waves from 100 Hz to 5 kHz near the equatorial plane between 5 and 8 R_E. We find a higher frequency of occurrence of chorus emissions than found in earlier surveys. We attribute this to the higher sensitivity of the SCATHA VLF receiver.

The most surprising feature of these maps is a general lack of wave activity in the 18-21 h local time sector. The diffuse aurora is a persistent feature of the aurora at the base of the field lines that thread this region. If we assume that the pitch-angle scattering mechanism responsible for the diffuse aurora is the same at all local times, we conclude that the electrons responsible for the diffuse aurora are not pitch-angle scattered by any type of plasma waves in the frequency range from 100 Hz to 5 kHz near the magnetic equator.

REFERENCES

Burtis, W. J., and R. A. Helliwell, Magnetospheric chorus: Occurrence patterns and normalized frequency, Planet. Space Sci., 24, 1007, 1976.

Christiansen, P. J., M. P. Gough, G. Martelli, J. J. Bloch, N. Cornilleau, J. Etcheto, R. Gendrin, D. Jones, C. Beghin, and P. Decreau, GEOS 1 observations of electrostatic waves and their relationship with plasma parameters, Space Sci. Rev., 22, 838, 1978.

Cornilleau-Wehrlin, N., R. Gendrin, F. Lefeuvre, M. Parrot, R. Grard, D. Jones, A. Bahnsen, E. Ungstrup, and W. Gibbons, VLF electromagnetic waves observed onboard GEOS-1, Space Sci. Rev., 22, 371, 1978.

Curtis, S. A., A theory for chorus generation by energetic electrons during substorms, J. Geophys. Res., 83, 3841, 1978.

Etcheto, J., R. Gendrin, J. Solomon, and R. Roux, A self-consistent theory of magnetospheric ELF hiss, J. Geophys. Res., 78, 8150, 1973.

Gough, M. P., P. J. Christiansen, G. Martelli, and E. J. Gershuny, Interaction of electrostatic waves with warm electrons at the geomagnetic equator, Nature, 279, 515, 1979.

Helliwell, R. A., J. P. Katsufrakis, T. F. Bell, and R. Raghuram, VLF line radiation in the Earth's magnetosphere and its association with power system radiation, J. Geophys. Res., 80, 4249, 1975.

Kaiser, T. R., A wave-particle-wave interaction observed on GEOS-2, in Proc. of Magnetospheric Boundary Layers Conf. (June 1979), European Space Agency Report ESA-SP 148, European Space Agency, Neuilly-sur-Seine, France, August, 1979.

Kennel, C. F., and M. Ashour-Abdalla, Electrostatic waves and the strong diffusion of magnetospheric electrons, Magnetospheric Plasma Physics, edited by A. Nishida, 245-344, Center for Academic Publications, Tokyo, Japan, 1982.

Koons, H. C., Role of hiss in magnetospheric chorus emissions, J. Geophys. Res., 86, 6745, 1981.

Koons, H. C., R. J. Maulfair, and J. C. Kordan, An atlas of spectrograms from the VLF receiver aboard the SCATHA (P78-2) spacecraft, ATR-81(7954)-2, The Aerospace Corporation, El Segundo, Calif., September, 1981.

Koons, H. C., Whistlers and whistler stimulated emissions in the outer magnetosphere, J. Geophys. Res., 90, 8547, 1985.

Kurth, W. S., J. D. Craven, L. A. Frank, and D. A. Gurnett, Intense electrostatic waves near the upper hybrid resonance frequency, J. Geophys. Res., 84, 4145, 1979.

Maeda, K., Cyclotron side-band emissions from ring-current electrons, Planet. Space Sci., 24, 341, 1976.

Mosier, S. R., M. L. Kaiser, and L. W. Brown, Observations of noise bands associated with the upper hybrid resonance by the IMP 6 radio astronomy experiment, J. Geophys. Res., 78, 1673, 1973.

Roeder, J. L., and H. C. Koons, A survey of electron cyclotron waves in the magnetosphere and the diffuse auroral electron precipitation, J. Geophys. Res., 94, 2529, 1989.

Tsurutani, B. T., and E. J. Smith, Postmidnight chorus: A substorm phenomenon, J. Geophys. Res., 79, 118, 1974.

Tsurutani, B. T., and E. J. Smith, Two types of magnetospheric ELF chorus and their substorm dependences, J. Geophys. Res., 82, 5112, 1977.

LABORATORY OPERATIONS

The Aerospace Corporation functions as an "architect-engineer" for national security projects, specializing in advanced military space systems. Providing research support, the corporation's Laboratory Operations conducts experimental and theoretical investigations that focus on the application of scientific and technical advances to such systems. Vital to the success of these investigations is the technical staff's wide-ranging expertise and its ability to stay current with new developments. This expertise is enhanced by a research program aimed at dealing with the many problems associated with rapidly evolving space systems. Contributing their capabilities to the research effort are these individual laboratories:

Aerophysics Laboratory: Launch vehicle and reentry fluid mechanics, heat transfer and flight dynamics; chemical and electric propulsion, propellant chemistry, chemical dynamics, environmental chemistry, trace detection; spacecraft structural mechanics, contamination, thermal and structural control; high temperature thermomechanics, gas kinetics and radiation; cw and pulsed chemical and excimer laser development, including chemical kinetics, spectroscopy, optical resonators, beam control, atmospheric propagation, laser effects and countermeasures.

Chemistry and Physics Laboratory: Atmospheric chemical reactions, atmospheric optics, light scattering, state-specific chemical reactions and radiative signatures of missile plumes, sensor out-of-field-of-view rejection, applied laser spectroscopy, laser chemistry, laser optoelectronics, solar cell physics, battery electrochemistry, space vacuum and radiation effects on materials, lubrication and surface phenomena, thermionic emission, photosensitive materials and detectors, atomic frequency standards, and environmental chemistry.

Electronics Research Laboratory: Microelectronics, solid-state device physics, compound semiconductors, radiation hardening; electro-optics, quantum electronics, solid-state lasers, optical propagation and communications; microwave semiconductor devices, microwave/millimeter wave measurements, diagnostics and radiometry, microwave/millimeter wave thermionic devices; atomic time and frequency standards; antennas, rf systems, electromagnetic propagation phenomena, space communication systems.

Materials Sciences Laboratory: Development of new materials: metals, alloys, ceramics, polymers and their composites, and new forms of carbon; nondestructive evaluation, component failure analysis and reliability; fracture mechanics and stress corrosion; analysis and evaluation of materials at cryogenic and elevated temperatures as well as in space and enemy-induced environments.

Space Sciences Laboratory: Magnetospheric, auroral and cosmic ray physics, wave-particle interactions, magnetospheric plasma waves; atmospheric and ionospheric physics, density and composition of the upper atmosphere, remote sensing using atmospheric radiation; solar physics, infrared astronomy, infrared signature analysis; effects of solar activity, magnetic storms and nuclear explosions on the earth's atmosphere, ionosphere and magnetosphere; effects of electromagnetic and particulate radiations on space systems; space instrumentation.